MOLECULAR PHYSICS REPORTS **38** (2003) 107-112

XPS SPECTRA, ELECTRONIC STRUCTURE AND ELECTRICAL RESISTIVITY OF YNi_4B COMPOUND

M. PUGACZOWA-MICHALSKA[1], G. CHEŁKOWSKA[2], T. TOLIŃSKI[1], A. KOWALCZYK[1]

[1]*Institute of Molecular Physics, Polish Academy of Sciences, Smoluchowskiego 17, 60-179 Poznań, Poland*

[2]*Institute of Physics, Silesian University, Uniwersytecka 4, 40-007 Katowice, Poland*

Abstract: The electronic structure of the ternary YNi_4B compound, crystallizing in the hexagonal $CeCo_4B$ structure (*P6/mmm* space group), was studied by X-ray photoelectron spectroscopy (XPS) and ab-initio calculations. The XPS valence band is compared with that obtained from *ab-initio* calculations. The temperature dependence of electrical resistivity can be described using the modified Bloch-Grüneisen relation.

1. INTRODUCTION

The RNi_4B compounds (R is a rare earth metal) crystallize in the hexagonal $CeCo_4B$ structure, which can be derived from RNi_5 by replacing two Ni atoms at the (2*c*) sites in every second layer by B atoms. In the $CeCo_4B$ structure the Ni atoms occupy two kinds of crystallographic sites, (2*c*) and (6*i*), the rare earth metal is also located in two sites, (1*a*) and (1*b*) and boron occupies one position (2*d*).

We have also performed researches on the RNi_4B compounds employing both magnetic measurements and X-ray photoemission spectroscopy (XPS) [1-6]. $CeNi_4B$ and $PrNi_4B$ appeared to be paramagnetic, but the former showed evidence of mixed valence and Kondo effect [6] and the latter composition exhibited evidence of Pr_2Ni_7 impurity phase. The remaining RNi_4B compounds were ferromagnetic, with exceptionally large coercive field in the case of $SmNi_4B$ (H_C = 7 T) [5].

For YNi_4B, Mazumdar et al. [7] observed paramagnetic behavior with an effective magnetic moment of about 0.2 μ_B/f.u. However, below 12 K superconductivity can appear in this compound [7]; this is usually ascribed to an additional phase containing carbon. The secondary phase does not exceed 2%. Our measurements of the temperature dependence of the magnetic *d.c.* susceptibility give also evidence of superconductivity with $T_C^S \approx 12$ K [4] and the superconducting phase contribution is about 2%. It is confirmed by the presence of the diamagnetic response in the magnetization process measured at 4.2 K.

The electronic structure of YNi_4B was calculated some years ago by Ravindran et al. in [8]. These calculations were carried out using the TB-LMTO method. The eigenvalues were obtained with a set of 64 *k*-points in the irreducible wedge of the first Brillouin zone of YNi_4B.

In this paper we present electronic and electrical resistivity studies of the YNi_4B compound.

2. EXPERIMENTAL DETAIL AND METHOD OF CALCULATION

The YNi_4B compound was prepared by the induction melting of stoichiometric amounts of the constituent elements in a water-cooled boat, under an argon atmosphere. The ingot was

inverted and melted several times to insure homogeneity. The crystal structure was established by a powder X-ray diffraction technique, using Cu-K_α radiation. The lattice constants are a = 4.987 Å and c = 6.948 Å.

The electrical resistivity was measured on a bar-shaped sample using a standard four-probe technique. The typical size of a sample was about 1 × 1 × 7 mm^3.

The X-ray photoemission (XPS) spectrum was obtained for the radiation with a photon energy of 1487.6 eV, from an Al-K_α source using a PHI 5700/660 Physical Electronics Spectrometer. The energy spectra of the electrons were analyzed by a hemispherical mirror analyzer with energy resolution of about ~0.3 eV. The Fermi level, E_F = 0, was referred to the gold 4*f*-levels binding energy at 84 eV. All emission spectra were measured immediately after breaking the sample in a vacuum of 10^{-10} torr.

The self-consistent spin-polarised Tight Binding Linear Muffin Tin Orbital (TB-LMTO) method within atomic sphere approximation (ASA) [9] was employed. The unit cell contains 12 atoms. The Vosko-Wilk-Nusair local exchange-correlation [10] potential was used. The computations were done for 750 k-points in the irreducible wedge of the first Brillouin zone.

3. RESULTS AND DISCUSSION

XPS has become a widely used technique for studying the valence and core bands in transition metal compounds. The experimental photoemission spectrum of the valence band region of YNi_4B is shown in Fig. 1 (solid line). The only peak is at 1.3 eV below E_F. The valence band spectrum exhibits the domination of Ni(3d) states at the Fermi level. The XPS valence spectrum is comparable with the results of our ab-initio calculations of the electronic structure of YNi_4B. The computed photoemission spectrum was obtained by weighting the density of states (DOS) with appropriate atomic cross sections for atomic photoemission and applying a convolution with a Lorentzian function, which accounts for the finite experimental resolution (σ = 0.4 eV).

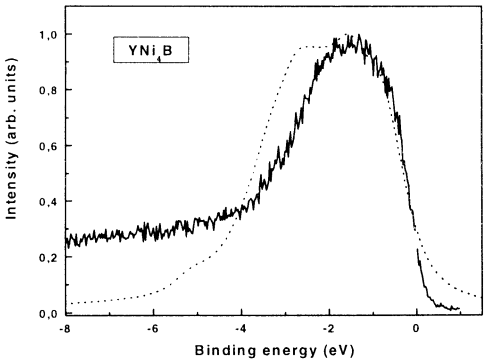

Fig. 1. Experimental (solid) and theoretical (dashed) valence band spectra of YNi_4B

The peaks of the XPS spectrum of YNi_4B at 870.3eV and 853eV were identified as Ni($2p_{1/2}$) and Ni($2p_{3/2}$) (Fig. 2). The spin-orbit coupling value determined from XPS spectra of these $2p_{1/2}$ and $2p_{3/2}$ bands is equal to 17.1 eV. The positions of these peaks are similar to those observed in pure nickel. A core-level photoemission spectrum of Y(3*d*) is presented in Fig. 3. The multiplet

structure of the Y(3d) state is visible. The positions of the peaks are in good agreement with metallic yttrium.

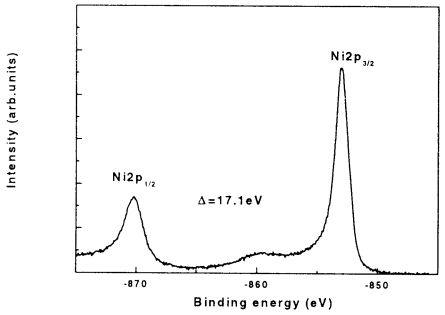

Fig. 2. Ni($2p_{1/2}$) and Ni($2p_{3/2}$) spectrum of YNi_4B

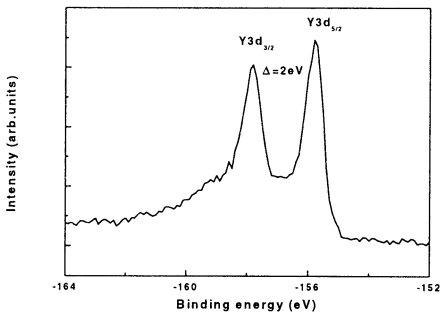

Fig. 3. Y($3d$) spectrum of YNi_4B

The ground state of YNi_4B is paramagnetic from electronic structure calculations. The total and partial DOS for YNi_4B are displayed in Fig. 4. The common feature of the electronic structure of RNi_4B (R = Ce or Gd) is the significant contribution of the d-states of Ni [1, 6].

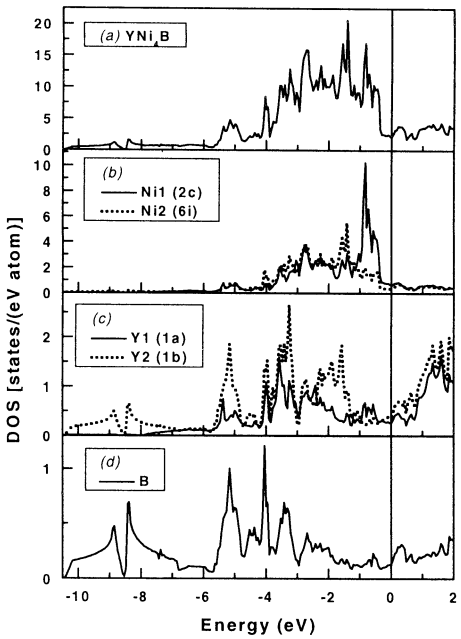

Fig. 4. The density of states of YNi_4B: (a) the total DOS in [states/(eV f.u.)], (b) the contribution of Y atoms in (1a) and (1b) sites; (c) the contribution of Ni atoms in (2c) and (6i) sites; (d) the contribution of B atoms

For the most part of the total DOS for YNi_4B we also observed the contributions of the Ni atoms in ($2c$) and ($6i$) positions, which contain mainly d-states of nickel below the Fermi level.

The different shapes of the partial DOS of Ni atoms in (2*c*) and (6*i*) positions (Fig. 4b) are caused by different types of atoms in the nearest neighborhood. The first peak below the Fermi level (-0.75 eV) is derived from *d*-states of Ni (2*c*). The second peak of the density of states observed at -1.4 eV is result of contributions both *d*-states of Ni(2c) and Ni(6i). The *d*-states of Y atoms give a small contribution (below 2 states/(eV cell)]) from the whole region from -6 eV to the Fermi level (0 eV). The total and partial DOS and the band structure of YNi_4B (Fig. 4) reveal the hybridisation of *d* states of Ni with d-states of Y and *p*-states of B. The DOS contribution of B atoms is visible below -7.5 eV.

The equilibrium volume and theoretical equilibrium lattice parameters are obtained from the minimum of total energy. The theoretical equilibrium lattice parameters are a = 5.143 Å and c = 7.165 Å. Thus, the theoretical values of lattice parameters are about 3.13% higher than the experimental ones. The density of states for YNi_4B is $N(E_F)$ = 4.25 states/(eV cell) and 4.79 states/(eV cell) for experimental lattice parameters and for lattice parameters from minimum of the total energy, respectively. The theoretical electronic specific heat coefficient γ, derived from $N(E_F)$ using the relation:

$$\gamma = \frac{\pi^2 k_B^2}{3} N(E_F) \tag{1}$$

(where k_B is the Boltzmann constant), is about 11.33 mJ/mol K^2 for the experimental lattice parameters a and c, and 12.75 mJ/mol K^2 for the lattice parameters from the minimum of total energy, respectively. These values of electronic specific heat coefficient are in good agreement with an earlier theoretical value of γ obtained from band calculations (12.96 mJ/mol K^2) by Ravindran et al. [8]. The theoretical obtained values of γ are smaller that the experimentally observed for YNi_4B (14.1 mJ/mol K^2) [12].

The total energy *versus* volume data were fitted to the six-term function, which was considered by Krasko and Olson in [13]:

$$E = E_1 + \frac{E_2}{V^{2/3}} + \frac{E_3}{V^{4/3}} + \frac{E_4}{V^{6/3}} + \frac{E_5}{V^{8/3}} + \frac{E_6}{V^{10/3}}, \tag{2}$$

Such a dependence of the total energy on atomic volume V is generated by the Murnaghan-Birch type equation of state [14] to obtain the bulk modulus. The bulk modulus B is defined by the equations:

$$B = -V\frac{\partial P}{\partial V} = V\frac{\partial^2 E}{\partial V^2}, \tag{3}$$

where E is the total ground-state energy as a function of volume, p is the pressure, and B is evaluated at the minimum of energy E. The bulk modulus is B_0 = 1.6 Mbar by our calculation.

The expression for Debye temperature Θ_D, as suggested by Moruzzi et al. [15],

$$\Theta_D = 41.63\left(\frac{r_0 B}{M}\right)^{1/2}, \tag{4}$$

where M is an atomic weight, r_0 is an atomic sphere radius, yields the value 272.89 K for YNi_4B.

Electrical-transport properties are very sensitive to the electronic structure as well as to the magnetic nature of the materials studied. The total resistivity of the magnetic compound can be written as:

$$\rho_m(T) = \rho_0 + \rho_{ph}(T) + \rho_m(T), \tag{5}$$

where ρ_0 is the residual resistivity, $\rho_m(T)$ is the magnetic contribution and $\rho_{ph}(T)$ is the contribution from the electron-phonon interactions. In Figure 7 the temperature dependence of resistivity for the paramagnetic YNi_4B compound is presented. Yttrium is not a rare earth however it is commonly included in the studies of RNi_4B series because YNi_4B creates the same hexagonal crystallographic structure as the RNi_4B compounds. At a temperature of 12 K a partial transition to superconductivity is noticeable, which is caused by the presence of the carbon-rich admixture [7]. From our measurements of the magnetic susceptibility [4] we estimated the amount of the superconducting phase at about 2%.

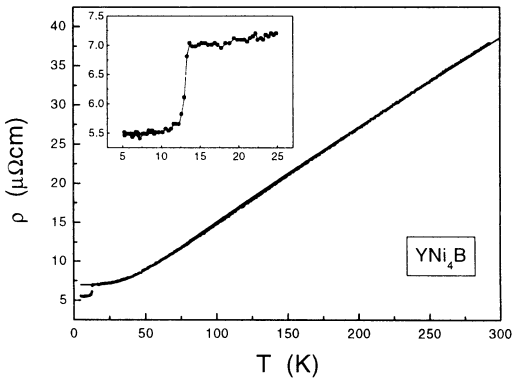

Fig. 5. The temperature dependence of the electrical resistivity for YNi_4B. Electrical resistivity $\rho(T)$ of YNi_4B fitted with Eq. (6). Inset shows the transition to superconductivity related to the impurity phase containing carbon

The $\rho(T)$ curve above the transition temperature can be well fitted using the modified Bloch-Grüneisen relation for metal-like compounds:

$$\rho(T) = \rho_0 + R\Theta_D\left(\frac{T}{\Theta_D}\right)^5 \cdot \int_0^{\Theta_D/T} \frac{x^5\,dx}{(e^x - 1)(1 - e^{-x})} \tag{6}$$

According to Matthiesen's rule the first term is a residual resistivity and the second term represents the phonon contribution. From the fit (solid line in Fig. 5) the residual resistivity is $\rho_0 = 6.98$ μΩcm, the constant $R = 0.109$ μΩcm/K and the Debye temperature $\Theta_D = 240$ K.

4. CONCLUSIONS

The electronic structure calculations have shown that YNi_4B is paramagnetic. Below the Fermi level the total DOS contained mainly *d* states of Ni atoms. The total, partial DOS and band structure of YNi_4B reveal the hybridisation *d* states of Ni with *d*-states of Y and *p*-states of B. The theoretical electronic specific heat coefficient γ derived from $N(E_F)$ is about 11.33 mJ/molK^2 for experimental lattice parameters. The obtained bulk modulus is $B_0 = 1.6$ Mbar. The theoretical calculations of the valence band are in good agreement with

the XPS spectrum. The valence band of the X-ray photoemission spectrum is composed mainly of the Ni($3d$) band.

The $\rho(T)$ curve above the transition temperature can be well fitted using the modified Bloch-Grüneisen relation. The experimental Debye temperature Θ_D is 240 K is in good agreement with calculated value (Θ_D = 273 K).

Acknowledgements

The work was supported by the Centre of Excellence for Magnetic and Molecular Materials for Future Electronics within the European Commission Contract No G5MA-CT-2002-04049.

References

[1] T. Toliński, M. Pugaczowa-Michalska, G. Chełkowska, A. Szlaferek, A. Kowalczyk, phys status sol. (b) **231**, 446 (2002).
[2] T. Toliński, A. Kowalczyk, A. Szlaferek, M. Timko, J. Kovac, Solid State Commun. **122**, 363 (2002).
[3] T. Toliński, G. Chełkowska, A. Kowalczyk, Solid State Commun. **122**, 145 (2002).
[4] T. Toliński, A. Kowalczyk, A. Szlaferek, B. Andrzejewski, J. Kováč, M. Timko, J. Alloys Comp. 34731 (2002).
[5] T. Toliński, A. Kowalczyk, G. Chełkowska, Physics Letters **A308**, 75 (2003).
[6] T. Toliński, A. Kowalczyk, M. Pugaczowa-Michalska, G. Chełkowska, J. Phys. Condens. Matter **15**, 1397 (2003).
[7] C. Mazumdar, R. Nagarajan, C. Godart, L. C. Gupta, M. Latroche, S. K. Dhar, C. Levy-Clement, B. D. Padalia, R. Vijayaraghavan, Sol, State Comm. **87**, 413 (1993).
[8] P. Ravindran, S. Sankaralingam, R. Asokamani, Phys Rev. **B52**, 12921 (1995).
[9] O. K. Andersen, O. Jepsen, M. Sŏb. In: *Yussouff MS editor. Electronic structure and Its Applications*, Springer, Berlin, p. 2 (1987).
[10] S. H. Vosko, L. Wilk, M. Nusair, Canadian Journal Phys. **58**, 1200 (1980).
[11] G. Hilscher, T. Holubar, N. M. Hohg, W. Perthold, M. Vybornov, P. Rogl, J. Magn. Magn. Mat. **140-144**, 2055 (1995).
[12] G. L. Krasko, G. B. Olson, Phys Rev. **B40**, 11536 (1989).
[13] F. D. Murnaghan, *Finite Deformation of an Elastic Solid*, Wiley, New York, 1951.
[14] V. L. Moruzzi, J. F. Janak, K. Schwarz, Phys Rev. **B37**, 790 (1988).